

# Automated Determination of Fingerprint Ridge Density and Fingerprint Size to Detect Sex Differences

Marleen Mohaupt<sup>1</sup>, Sieke Stoeter and Dirk Labudde<sup>1</sup>

**Abstract.** A fingerprint is probably the most important biometric feature when trying to link a suspect to a crime scene. So far, without a hit in a fingerprint database, it was impossible to use a collected fingerprint to narrow down the group of suspects. Moreover, in the existing studies about deriving phenotypic characteristics from fingerprints the analyses were done manually. In contrast, in this paper a procedure is presented to automatically determine the fingerprint ridge density and the fingerprint size, in order to derive information about the sex of the person the fingerprint belongs to. All 10 fingerprints of 140 individuals (70 males and 70 females) belonging to the German Caucasian population were secured and then analyzed. The best result was obtained for the ulnar area in combination with the fingerprint size of the left thumb with  $F_1$  measures of 0.84 (k-nearest neighbors algorithm - KNN), 0.833 (Support Vector Machine) and 0.817 (logistic regression).

**Keywords:** Fingerprints, Ridge Density, Sex Classification.

## 1 Introduction

In forensics, fingerprints are the best-known pieces of evidence [1]. Overall, a fingerprint contains three levels of information [2]. The first level detail is the presence of one of the three basic patterns (loop, whorl or arch) [2]. Other anatomical features, the minutiae, e.g. interruptions and branches, are the second level details [2]. Furthermore, the third level details include special features, such as scars, creases or pores [2-4].

Without a hit in a fingerprint database such as the Automated Fingerprint Identification System (AFIS) from INTERPOL, it is impossible to use a collected fingerprint to narrow down the group of suspects, e.g. by sex, solely based on dactyloscopic evidence. In 1999 Mark A. Acree developed a method for determining the ridge density (RD - the number of ridges in a well-defined square) [5], which formed the basis for numerous subsequent studies [6-9]. It was found that the RD depends on several factors: age [5, 10, 11], population, sex [6] and the position of the well-defined area within the fingerprint. However, determining the RD manually is time-consuming and depends on the subjective view of an expert. In this paper, we present a novel approach, which performs this task automatically. As a result, a larger data set can be analyzed in a shorter amount of time.

---

<sup>1</sup> University of Applied Sciences Mittweida, Technikumpl. 17, 09648 Mittweida, marleen.mohaupt@hs-mittweida.de/ dirk.labudde@hs-mittweida.de

## 2 Related Works

As demonstrated in various studies [5-9] the ridges in fingerprints of females are closer together and, thus, show a higher RD compared to men. Depending on the location of the measurements (count areas) and the population of the suspects, the discriminant threshold to determine the sex differs. In most papers, these thresholds were determined using Bayes' theorem for both sexes. For a Spanish population, for the radial area, the fingerprint is more likely to be assigned to a male at a density of  $< 16$  lines/  $25 \text{ mm}^2$  and more likely to be assigned to a female at a density of  $16$  lines/  $25 \text{ mm}^2$  or more. The average values vary due to different populations and the location of the count area.

For the Punjabi population in India Dhall and Kapoor chose a discriminant function and logistic regression to determine the sex. The results of five areas to measure the RD were analyzed and an accuracy of 97.4% using logistic regression was obtained. When the areas are considered individually, an accuracy of 87.2 % is calculated for the radial areas and 82.9 % for the ulnar areas. [6]

Verma and Agarwal, using only the RD without a clear definition of the selected area, achieved a classification rate of 53% using a SVM classifier. Their precision was improved by incorporating additional features. They additionally calculated the ridge thickness to valley thickness ratio and the ridge width and achieved an accuracy of 59.5 % and 68 %, respectively. Using all three features, an accuracy of 91 % was achieved. [12]

Badawi et al. used five features: ridge count, white lines count, ridge thickness to valley thickness ratio, ridge count asymmetry, and pattern type concordance. The ridge thickness to valley thickness ratio was calculated automatically for the scanned ink fingerprints by dividing the image into  $30 \times 30$  pixel non-overlapping squares and determining the value for each block. Then, the average for all blocks was calculated. Blocks with low image quality were automatically excluded. All other features were determined manually. Three models were created with Fuzzy C- Means. With a linear discriminant analysis, they achieved an accuracy of 86.5 % and a slightly higher accuracy of 88.5 % using a multilayer backpropagation neural network. [13]

In another study (see [11]), fingerprint ridge count and fingertip size (FPS) of an Indian population were determined. The ridge count consists of three parameters: the number of lines located on the straight line between the core point and the delta, and the lines located on the diagonals at  $45^\circ$  and  $135^\circ$  beginning at the core point for the entire area of the fingerprint. The FPS was determined by the Fingkey Hamster II scanner. For the optimal score assignment method, the most frequent values were used as a reference for determining a score for fingerprint ridge count and FPS. Afterwards, a score for male and female was determined from the sum of both values. If the male score was higher than the female score, the fingerprint is most likely from a male, otherwise from a female. Using optimal score assignment, an accuracy of 88.41% was obtained for the right ring finger. [11]

For the analysis of large data sets, parameters for sex differentiation should be determined automatically. In this study, both RD and fingerprint size were automatically determined as possible parameters for sex differentiation and evaluated accordingly.

### 3 Materials and Methods

During the data acquisition, 1400 fingerprints of 70 females and 70 males were taken. The age of the subjects varied between 19 and 38 years (mean: 22.36, SD: 3.91). Since the RD depends on ethnicity, the study was performed exclusively for Caucasians residing in Germany. We have requested the biological sex and not the gender identity of the subjects (see [14]). Fingerprints were acquired by using a VERIFIER 300 LC 2.0 (CROSS MATCH) finger scanner. From each subject the prints of all 10 fingers were taken, starting with the little finger of the left hand and ending with the little finger of the right hand. Each image has a horizontal and vertical resolution of 500 dpi, matching the FBI standard for forensic applications in order to reliably extract all ridges and minutiae with a dimension of 640x480 pixels. Several studies indicate that arch patterns are observed in about 5 % of all fingerprints while loop patterns occur in about 60 – 70 % of all fingerprints and whorls about 30 % [15-17]. This distribution could also be observed in the data set.

#### 3.1 Determination of the Ridge Density

In order to automatically determine the RDs, a MATLAB [18] program was implemented. Additional modules for image segmentation [19] and enhancement [20] were utilized. Eight steps were applied to each scanner image before the RD was determined (see Fig. 1). Since the determination of the RD requires closed ridges, some special features, such as scars, were closed by the image processing methods used. This represents a loss of information, that was, however, insignificant with respect to classification performance.

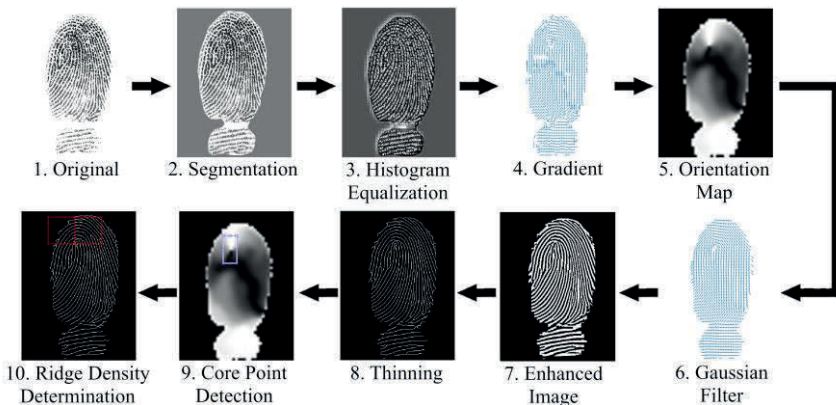


**Fig. 1.** Automated ridge density estimation, requires the reliable location of the fingerprint core. To that end, multiple image pre-processing steps are involved prior to core detection.

*Segmentation*, which separates the actual fingerprint from the background, was used to remove artefacts that occur during the scanning process. This method was developed and published by Fahmy and Thabet [19].

In the scanned fingerprint, the intensity of the grey values varies greatly, so that many papillary lines are only faintly visible. Image enhancement highlights, connects and evenly colors the lines so that the program can capture each line. Bifurcations and ending lines are not altered in the process. Islands are also preserved in the enhanced image. For the enhancement, the algorithm implemented by Houjun Jiang [20] was adopted and only the block size changed. Since local operations give a better result than the global processing of the whole image, the fingerprint was divided into several non-overlapping blocks and improved systematically. Fig. 1 above shows the effect of each step on a fingerprint scan. In the enhanced image, it can be seen that pores are no longer visible. In other scanner images, scars and wrinkles are no longer displayed and all lines are closed. Only the furrow of the first phalanx can be seen in many enhanced images.

The variations in grey levels are due to the varying pressure of the finger on the scanner. In order to simplify further image analysis, the contrast of non-high contrast areas had to be increased. This can be realized by using *histogram equalization* ("histeq" function). This involved stretching the intensity of the pixels analyzed in the histogram so that the differences between dark pixels (lines) and light pixels (valleys) are better emphasized. This also achieved an increase in contrast. A desirable side effect was the removal of visible sweat pores. However, scars and wrinkles were still visible after this step. Next, the gradient image was created. This step is necessary for the creation of the orientation map and the detection of the edges. The gradient indicates the strength of the change in direction of a mathematical function. With a small gradient value and, thus, a small change in direction, the papillary lines run parallel to the calculated line course. To obtain more uniform lines in the enhanced image, the gradient image is smoothed. For this purpose, the *Gaussian filter* with a block size of 5x5 pixels was used. However, this can cause the areas where the direction of the lines is not constant to be incorrect. This mainly affects the areas immediately around the core point and the delta. Therefore, some fingerprints may have slight artefacts that are more noticeable after thinning. This problem is addressed when counting the lines. To further highlight the papillary lines, a bandpass filter was applied. The Gabor filter is based on sinusoidal frequencies created using the Gaussian function ("imgaborfilt" function) which extracts and highlights the papillary lines with a block size of 32. This allows areas with a strong structural change to be captured and enhanced. The gradient image was also used to create an *Orientation Map*. The average change in direction was calculated for each block. The larger the value the darker is the area. Since the curvature of the ridges is strongest around the core point, a characteristic line was obtained in the orientation map, at which upper end the core point is located [21]. To simplify the counting of fingerprint lines, the lines in the enhanced image are reduced to a width of one pixel, using common *thinning* techniques and an inversion. To do so, the internal MATLAB [18] function *bwmorph* was used. The procedure described in [10] of setting squares to determine the RD directly above the core point was also applied here. Bahgat et al. used the orientation map and discovered that the image values around the core point follow a certain pattern: In the neighboring pixels, the change in direction increases from almost 0° to almost 180° anti-clockwise [21]. This *core point detection* was extended by using template matching to process the different types of orientation maps for the basic

patterns. Furthermore, a cross-correlation was carried out to detect the area of the orientation map that most closely matches one of four templates due to the different orientation maps of the ridge patterns. The center of the template corresponds to the core point of the fingerprint. For the left hand, the left square corresponds to the ulnar and the right square to the radial area. For the right hand, the assigned areas are reversed [10]. For the *RD determination*, the lines that intersect an imaginary diagonal of the respective square i.e. white pixels on this line should be counted (see Fig. 2). To detect all lines, neighbors of black pixels on the diagonal also had to be checked for white pixels. Possible additional pixels, which could result from the image enhancement, were only interpreted as one line. For this purpose, white pixels on the straight line with a distance less than or equal to three were counted as one line. Unfortunately, some fingerprint were not fully captured. Thus, the squares reach over the fingerprint, resulting in a lower RD. To use it anyway, the distance between the last found line and the upper square corner is determined, and additional lines are estimated using the median of the given ridge distances (see Fig. 2).

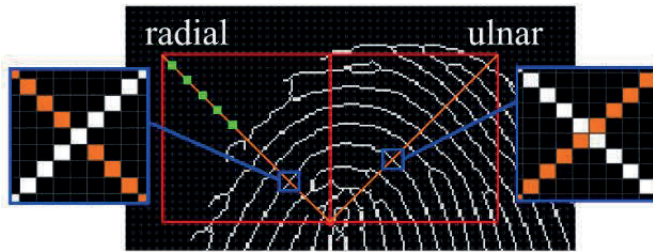


**Fig. 2.** Magnification of the intersections of the papillary lines (white) with the imaginary diagonal (orange) of the radial and ulnar regions (red) for fingers of the right hand and intersections with the estimated lines (green dots)

In the left magnification (blue), the white dot lies directly on the diagonal and is evaluated as a papillary line. In the right magnification (blue), the white pixels of the papillary line are not on the diagonal. Therefore, for black pixels, the top three neighboring pixels were checked for a white color value. After each hit, the following pixel on the diagonal was skipped to avoid double counting of lines.

### 3.2 Determination of the Fingerprint Size

As a second parameter to differentiate the sex, the fingerprint size (FPS) was determined to approximate the fingertip size. For its determination, the segmentation mask from the first step was used. The segmented area of the fingerprint was displayed in white pixels while the background was dyed black. Since there are significantly more artefacts in some images, which are not removed by the segmentation function in every case, the brightness of the image was increased. The FPS was calculated with the following formula:

$$fingerprint\ size = \frac{Number\ of\ white\ pixels * 25.4^2}{dpi^2}. \quad (1)$$

## 4 Results

1272 of 1400 core points were detected correctly, which corresponds to an overall accuracy of 90.85 %. The automatic core point detection shows an accuracy of 95.31 % for whorls, 91.29 % for loops and 87.61 % for arches. The orientation maps of plain arches do not show strong gradient changes and, therefore, the core point is difficult to find with the used templates. Hence, an adaptation of the core point detection for this specific problem is needed. The core point serves as a reference point for locating the squares with the chosen size of 75x75 for the radial and ulnar areas. Additionally, 27 fingerprints were incomplete and the squares covered an area outside the actual fingerprint, therefore the missing epidermal ridges had to be estimated.

For the male subjects a mean ridge density of 12.60 (1.82) was calculated in the radial and 12.56 (2.07) in the ulnar area. For the female subjects a mean value of 13.80 (2.00) in the radial and 13.71 (2.04) in the ulnar area were obtained. The exact distribution of the RD is visualized in Fig. 4. The values range from 7 to 19 with a mode of 12 (radial) and 7 to 20 with a mode of 13 (ulnar) in the male group. For the females the values are between 7 and 20 with a mode of 13 (radial) and 8 and 20 with a mode of 14 (ulnar). Overall, it can be seen that women have a higher ridge density than men for both radial and ulnar values and a statistically significant difference was observed (Mann-Whitney-U test,  $p < 0.05$ ). However, the distribution of the RD for both sexes overlap. Instead of using a single threshold value to assign the correct sex, logistic regression, SVM and KNN were used to predict the sex. To increase the probabilities, a second feature was determined. The surface area of the segmentation mask was calculated in  $\text{mm}^2$  for each fingerprint. For males, the values range from  $102 \text{ mm}^2$  to  $372 \text{ mm}^2$  with a mode of  $203 \text{ mm}^2$  and a mean value of  $201.45 \text{ mm}^2$ . For females, the values range from  $94 \text{ mm}^2$  to  $349 \text{ mm}^2$  with a mean value of  $168.49 \text{ mm}^2$  and a mode of  $145 \text{ mm}^2$ .

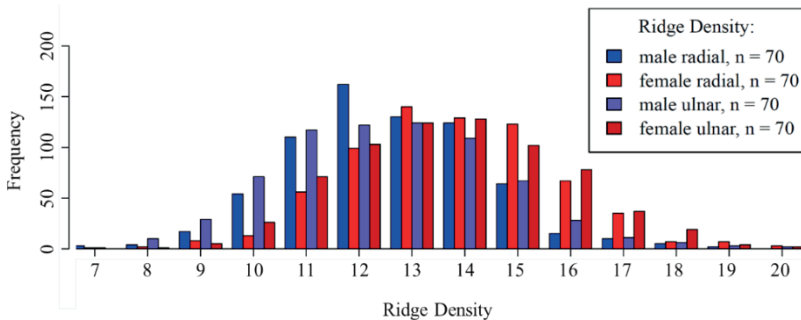


**Fig. 3.** Frequency distribution of the RD in the ulnar and radial area for the subjects

A logistic regression (LR) model and several support-vector machine (SVM) models were trained to classify and predict the sex. Additionally, the classic k-nearest neighbors algorithm (KNN) was used in order to evaluate the baseline classification performance. With  $k = 11$  k-NN, LR and SVM models were trained and tested using a 10-fold cross validation. The experimental results show that with only one feature of the RD, the classification

rate is quite low. For the test data set, the best value for the radial RD was obtained for the right middle finger with an accuracy of 66.6 % and an  $F_1$  measure of 0.666 using LR. For the ulnar RD the accuracy was 64.57% and the  $F_1$  measure 0.717. For the left thumb, which provided the best results for the analyses with the FPS, the accuracy for the radial RD was 59.66 %. However, the  $F_1$  measure was only 0.609. For the ulnar RD, both the accuracy with 63.98 % and the  $F_1$  measure of 0.653 were slightly higher. The values calculated with the SVM and the KNN do not deviate much from the other values (see Table 1). Overall, the results improved when adding FPS as a feature.

**Table 1.** Classification Accuracy (A) and  $F_1$  measure ( $F_1$ ) for the Fingerprint Size (FPS), the radial RD (rRD) and ulnar RD (uRD) using LR, SVM and KNN algorithm

Finger	FPS		rRD		uRD		rRD+uRD+FPS		uRD+FPS	
	A [%]	$F_1$	A [%]	$F_1$	A [%]	$F_1$	A [%]	$F_1$	A [%]	$F_1$
1 (LR)	67.37	0.707	64.04	0.612	55.12	0.572	73.57	0.758	71.77	0.744
2 (LR)	73.68	0.767	67.35	0.627	57.99	0.589	73.37	0.766	73.39	0.753
3 (LR)	74.35	0.768	65.55	0.648	66.87	0.666	73.06	0.752	74.68	0.771
4 (LR)	67.17	0.704	60.43	0.599	58.85	0.588	69.12	0.711	68.61	0.715
5 (LR)	76.35	0.784	59.66	0.589	63.98	0.636	78.13	0.786	<b>79.58</b>	<b>0.817</b>
6 (LR)	76.88	0.775	61.86	0.604	56.25	0.577	78.23	0.794	74.52	0.768
7 (LR)	73.87	0.763	62.93	0.598	57.75	0.561	70.94	0.724	70.07	0.728
8 (LR)	68.53	0.734	66.60	0.650	64.57	0.674	66.88	0.695	65.20	0.685
9 (LR)	67.26	0.712	63.26	0.625	54.50	0.563	70.41	0.738	70.11	0.733
10 (LR)	68.42	0.719	61.31	0.627	59.67	0.556	72.68	0.750	74.35	0.762
1 (KNN)	67.80	0.701	57.13	0.560	55.24	0.611	68.14	0.687	71.76	0.735
2 (KNN)	71.28	0.735	61.65	0.673	58.98	0.514	73.58	0.751	68.09	0.711
3 (KNN)	72.44	0.671	59.83	0.633	63.97	0.661	73.97	0.742	66.47	0.658
4 (KNN)	64.43	0.655	64.03	0.652	65.15	0.661	69.30	0.715	65.92	0.700
5 (KNN)	72.94	0.754	57.13	0.552	69.01	0.624	79.03	0.802	<b>82.37</b>	<b>0.840</b>
6 (KNN)	73.32	0.754	53.84	0.552	51.67	0.523	74.70	0.762	76.36	0.749
7 (KNN)	74.75	0.757	62.42	0.640	45.00	0.497	71.49	0.739	64.48	0.655
8 (KNN)	68.12	0.692	65.38	0.703	63.59	0.658	66.90	0.691	60.12	0.629
9 (KNN)	68.23	0.727	62.53	0.608	62.16	0.634	69.54	0.722	69.71	0.725
10 (KNN)	66.79	0.696	54.79	0.596	47.89	0.551	69.54	0.725	69.15	0.729
1 (SVM)	72.67	0.749	60.73	0.613	54.79	0.507	73.69	0.767	70.08	0.729
2 (SVM)	73.26	0.750	64.81	0.681	61.73	0.641	74.75	0.779	73.26	0.754
3 (SVM)	74.05	0.770	63.00	0.632	60.96	0.605	73.04	0.734	69.48	0.705
4 (SVM)	66.93	0.649	60.48	0.6406	61.69	0.629	72.65	0.722	71.54	0.696
5 (SVM)	75.36	0.781	60.15	0.612	72.26	0.719	<b>82.56</b>	<b>0.833</b>	<b>80.51</b>	<b>0.832</b>
6 (SVM)	75.79	0.784	60.29	0.597	56.95	0.551	75.67	0.766	74.50	0.748
7 (SVM)	74.13	0.756	65.51	0.674	55.41	0.554	69.79	0.681	69.18	0.728
8 (SVM)	68.07	0.694	64.45	0.615	56.10	0.590	70.50	0.729	71.68	0.728
9 (SVM)	67.92	0.711	62.45	0.584	64.11	0.646	70.63	0.701	68.38	0.690
10 (SVM)	70.73	0.741	64.14	0.618	59.89	0.590	74.29	0.714	73.21	0.737

Figure 4 shows that the FPS given in  $\text{mm}^2$  is higher for males than for females. The statistically significant difference in size resulted in a higher classification probability especially for the thumbs: for the left thumb, an accuracy of 76.35 % and an  $F_1$  measure of 0.784 were calculated and for the right thumb, an accuracy of 76.88 % and an  $F_1$  measure of 0.775 were estimated with LR (see Table 2). Thus, for the FPS a better prediction could be made than for the RD. However, the best results were obtained by combining both features. For the ulnar RD and FPS, an accuracy of 79.58 % and an  $F_1$  measure of 0.817

were calculated for the left thumb using LR. The SVM increased the accuracy to 80.51 % and the  $F_1$  measure to 0.832. The highest value was achieved with the KNN with an accuracy of 82.37 % and an  $F_1$  measure of 0.84, which could not be exceeded even by the additional use of the radial RD.

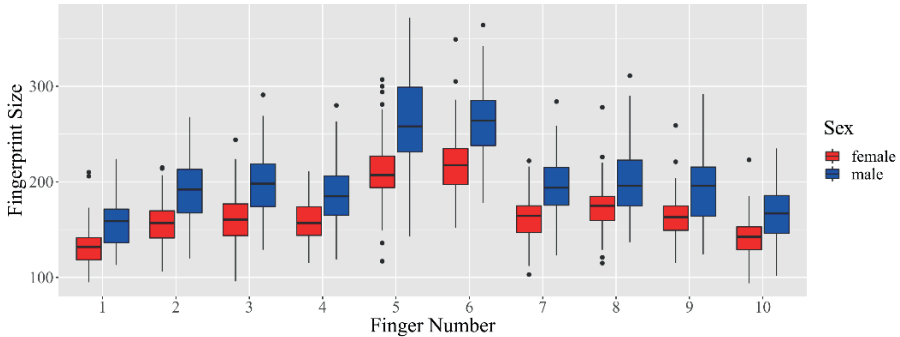


**Fig. 4.** Per-finger FPS distributions of all 140 subjects.

**Table 2.** Mean (meanFPS) and median fingerprint size (medianFPS) for each finger

Finger	meanFPS [mm <sup>2</sup> ] (SD) males	females	medianFPS [mm <sup>2</sup> ] (IQR) males	females
1	159.4 (26.6)   133.3 (21.8)		159.0 (35.0)   132.0 (23.0)	
2	190.3 (35.2)   156.1 (22.7)		192.0 (45.5)   157.0 (28.5)	
3	196.4 (37.1)   163.1 (28.2)		198.0 (44.5)   160.5 (33.3)	
4	187.4 (49.2)   159.0 (22.2)		185.0 (44.8)   157.0 (29.8)	
5	261.1 (41.8)   212.1 (35.8)		258.0 (67.5)   207.0 (33.0)	
6	263.7 (31.4)   219.8 (33.0)		264.0 (47.0)   217.5 (37.5)	
7	194.4 (34.3)   161.8 (24.2)		194.0 (39.5)   164.5 (28.0)	
8	201.3 (36.6)   172.9 (26.4)		196.0 (47.8)   175.0 (25.3)	
9	193.8 (29.3)   165.0 (23.5)		196.0 (51.3)   163.0 (25.5)	
10	166.8 (26.6)   141.2 (21.1)		167.0 (39.5)   142.5 (24.0)	

## 5 Discussion

Within this study, an automatic determination of the fingerprint ridge density and the fingerprint size, to derive information about the sex of the person the fingerprint belongs to, has been implemented. Dhall and Kapoor achieved a classification accuracy of 97.4%, by using five areas for the determination of the RD [6]. For our dataset, only the radial and ulnar regions could be used because the fingerprints were taken without rolls and, thus, the area to be analyzed is much smaller. Considering only the RD, Verma and Agarwal's value of 53% [12] could be raised to an average value of 63.29% (LR), 62.60 % (SVM) and 59.87% (KNN) for the radial region and 59.55% (LR), 60,38 % (SVM) and 58.26% (KNN) for the ulnar region. Their other features such as ridge thickness to valley thickness ratio (59.5 %) and ridge width (68 %) are also below the classification probability from

the FPS of 71.38 % (LR), 71.89 % (SVM) and 70.01 % (KNN) [12]. Combining the features, the result of Verma and Agarwal dominates. Ganasivam and Vijayarajan did not perform analyses for the individual features. Their top result of 88.41% includes three measurements for the manually determined ridge count and FPS [11].

In this study as expected, the FPS of males are on average larger than those of females and a statistically significant difference could be demonstrated, especially for the thumbs. However, many outliers could be observed. The broad distribution could indicate larger fingertips or even fingerprints with poor quality. Artifacts that were not removed during segmentation may extend the area beyond the actual fingerprint, resulting in a higher value. It is possible that the particularly large fingerprints are due to tall subjects with large hands and fingers. With only two measurements, our best result was an accuracy of 82.37% and an  $F_1$  measure of 0.84 (KNN) for the right thumb. This result is better than that of Badawi et al. using Fuzzy C- Means, which achieved an accuracy of 80.39%. However, their best result using backpropagation multi-layer neural networks is an accuracy of 88.5% [13]. In the publications, it appears that a good result could not be obtained with only one feature [6, 11, 13]. To improve our predictive performance, another method like calculating the ridge count and ridge thickness should be implemented. The use of methods to determine the location of fingerprints on objects via photogrammetry or scanning techniques should also make it possible to determine features i.e. the hand geometry [22]. With this information, sex assignment can be improved and possibly further phenotypic characteristics can be derived.

Overall, connecting the fingerprint evidence to other evidence including biometric information found at a crime scene, such as footprints, can help improve the reconstruction of the crime scene depending on the location of the evidence. Furthermore, this method cannot be used to on its own to identify a person. However, in combination with other evidence it can be used to determine the sex of the suspect. With the help of sex differentiation, the group of persons can at least be narrowed down.

## 6 Conclusion

Within this study, a program for automatic fingerprint RD and FPS estimation was implemented. So far, this is only an estimate - an analysis and comparison of a manual analysis and the automated analysis is still required. A main part was the automatic detection of the core point (overall accuracy of 90.85 %) to define the regions for calculating the number of epidermal ridges. Furthermore, by estimating the RD, it is possible to analyze fingerprints resulting in an easier and faster analysis in comparison to the manual approaches. So far, studies using manual assessment have shown that the RDs of men and women differ. Within this study, similar results were achieved, using an automatic procedure. The best values were obtained using the RD of the ulnar region and the FPS for the left thumb with an  $F_1$  measure of 0.817 (LG), 0.832 (SVM) and 0.840 (KNN). The results of the presented study support the hypothesis that woman have a higher RD than men and smaller fingertips as presented in former studies.

## 7 References

1. Datta, A. K.: *Advances in fingerprint technology*. 1st edn. CRC press, Boca Raton (2001).
2. U.s. Department of Justice: *The Fingerprint Sourcebook*. CreateSpace Independent Publishing Platform, USA (2014).
3. Jain, A., Chen, Y., Demirkus, M.: Pores and Ridges: Fingerprint Matching Using Level 3 Features. 18th International Conference on Pattern Recognition, (2006).
4. Khan, M. A. et al.: A spatial domain scar removal strategy for fingerprint image enhancement. *Pattern Recognition* (60), 258-274 (2016).
5. Acree, M. A.: Is there a gender difference in fingerprint ridge density? *Forensic science international* 102(1), 35-44 (1999).
6. Dhall, J. K., Kapoor, A. K.: Fingerprint Ridge Density as a Potential Forensic Anthropological Tool for Sex Identification. *Journal of Forensic Sciences* 61(2), 424-429 (2016).
7. Gutiérrez-Redomero, E., et al.: Variability of fingerprint ridge density in a sample of Spanish Caucasians and its application to sex determination. *Forensic Science International* 180(1), 17-22 (2008).
8. Gutiérrez-Redomero, E., et al.: A comparative study of topological and sex differences in fingerprint ridge density in Argentinian and Spanish population samples. *Journal of Forensic and Legal Medicine* 20(5), 419-429 (2013).
9. Kapoor, N., Badiye, A.: Sex differences in the thumbprint ridge density in a central Indian population. *Egyptian Journal of Forensic Sciences* 5(1), 23-29 (2015).
10. Sánchez-Andrés, A., et al.: Impact of aging on fingerprint ridge density: Anthropometry and forensic implications in sex inference. *Science & Justice* 58(5), 323-334 (2018).
11. Gnanasivam, P., Vijayarajan, R.: Gender classification from fingerprint ridge count and fingertip size using optimal score assignment. *Complex & Intelligent Systems* 5(3), 343-352 (2019).
12. Verma, M., Agarwal, S.: Fingerprint based male-female classification. *Cisis* 53, 251-257 (2008).
13. Badawi, A. et al.: Fingerprint based gender classification. *The international conference on image processing. Computer vision and pattern recognition* 1, 41-46 (2006).
14. Tannenbaum, C. et al.: Sex and gender analysis improves science and engineering. *Nature*, 575(7781), 137-146 (2019).
15. Patil, V., Ingle, D. R.: An association between fingerprint patterns with blood group and lifestyle based diseases: a review. *Artif Intell Rev* 54, 1803–1839 (2020).
16. Henry, E. R.: *Classification and uses of fingerprints*. George Rutledge and Sons Ltd, London 1900.
17. Galton, F.: *Fingerprints*. Macmillan, London (1892).
18. MATLAB. version 7.10.0 (R2010a). Natick, Massachusetts: The MathWorks Inc. (2010).
19. Fahmy, M. F., Thabet, M. A.: A fingerprint segmentation technique based on morphological processing. In *IEEE International Symposium on Signal Processing and Information Technology*, 000215-20 (2013).
20. Haojun, J.: *Fingerprint Image Enhancement*, <https://github.com/jianghaojun/Fingerprint-Image-Enhancement>, last accessed 2020/03/11.
21. Bahgat, G. A. et al.: Fast and accurate algorithm for core point detection in fingerprint images. *Egyptian Informatics Journal* 14, 15-25 (2013).
22. Becker, S. et al.: Comprehensive Framework for High Resolution Image-based 3D Modeling and Documentation of Crime Scenes and Disaster Sites. *International Journal On Advances in Systems and Measurements*, 11 (2), 1-12, 2018